IOPscience iopscience.iop.org

Home Search Collections Journals About Contact us My IOPscience

Cathodoluminescence study of Si complex formation in self-doped and intentionally Si-doped GaAs conformal layers

This article has been downloaded from IOPscience. Please scroll down to see the full text article.

2004 J. Phys.: Condens. Matter 16 S99

(http://iopscience.iop.org/0953-8984/16/2/012)

View the table of contents for this issue, or go to the journal homepage for more

Download details:
IP Address: 129.252.86.83
The article was downloaded on 28/05/2010 at 07:15

Please note that terms and conditions apply.

INSTITUTE OF PHYSICS PUBLISHING JOURNAL OF PHYSICS: CONDENSED MATTER
J. Phys.: Condens. Matter **16** (2004) S99–S106 PII: S0953-8984(04)66996-7

Cathodoluminescence study of Si complex formation in self-doped and intentionally Si-doped GaAs conformal layers

O Martínez[1,6], A M Ardila[2], M Avella[1], J Jiménez[1], F Rossi[3], N Armani[3], B Gérard[4] and E Gil-Lafon[5]

[1] Departamento Física de la Materia Condensada, ETSII, University of Valladolid, 47011 Valladolid, Spain
[2] Departamento Física, Facultad de Ciencias, Universidad Nacional de Colombia, Ciudad Universitaria, Santa Fe de Bogotá, Colombia
[3] CNR-IMEM Institute, Parco Area delle Scienze 37/A, I-43010 Località Fontanini, Parma, Italy
[4] THALES, Corporate Research Laboratory, 91404 Orsay Cedex, France
[5] LASMEA UMR CNRS 6602, Université Blaise Pascal, Les Cézeaux, 63177 Aubiére Cedes, France

E-mail: oscar@fmc.uva.es

Received 31 July 2003
Published 22 December 2003
Online at stacks.iop.org/JPhysCM/16/S99 (DOI: 10.1088/0953-8984/16/2/012)

Abstract
An Si complex formation is observed in unintentionally doped as well as n-type doped GaAs layers grown laterally on GaAs seeds deposited on (100) Si substrates. The free carrier concentration was accurately assessed by previous Raman studies. Particularly interesting was the observation of a doped stripe nearby the GaAs seed in the unintentionally doped layers. In this work the formation of the complexes in both kinds of doped samples was analysed by means of SEM-cathodoluminescence (CL) studies. Different bands, indicative of the presence of more than one Si-related transition, have been observed in the infrared spectral region. The distribution of some of the related complexes at the different depths along the growth axis was analysed by depth-resolved CL. The nature of the emission levels has been investigated by power dependent CL studies, allowing to correlate them to DAP transitions. The Si autodoping origin of the doped stripes on the unintentionally doped samples was also confirmed.

(Some figures in this article are in colour only in the electronic version)

1. Introduction

The integration of GaAs with Si, very attractive since it combines the low-cost technology and the mechanical strength of silicon with the higher optoelectronic performance of the gallium

[6] Author to whom any correspondence should be addressed.

© 2004 IOP Publishing Ltd Printed in the UK

arsenide, is up to now a highly challenging issue. Many efforts have been made in the last decades, which have led to some progress [1, 2]. The main problems of growing GaAs on Si are the large lattice (4%) and the thermal (55%) mismatch between Si and GaAs, as well as the difficulties of growing a polar semiconductor on a non-polar one, leading to a high quantity of defects in the grown layers, particularly threading dislocations [3]. Different deposition techniques and treatments have been proposed to improve the quality of the layers, such as annealing [2], insertion of buffer layers in vertical growth [4] or passivating layers in lateral growth [5]. In spite of this, the density of crystal defects does not decrease enough to render these structures suitable for reliable optoelectronic applications. Pribat *et al* [6] proposed an effective method, called 'conformal', to produce GaAs layers on Si substrates.

In the conformal growth method [6, 7] a GaAs buffer layer is conventionally grown on a silicon wafer, giving dislocation densities as high as 10^7–10^8 cm^{-2}. This GaAs layer is then coated with a dielectric cap layer (Si_3N_4 or poly-Si), on which windows are periodically opened. The GaAs under the dielectric is then selectively etched, preserving only some parallel stripes of GaAs that will play the role of seeds. The conformal layers are grown laterally from these seeds by either hydride vapour phase epitaxy (HVPE) or metal organic vapour phase epitaxy (MOVPE). Thus, a confined epitaxial growth seeding at the (110) faces of the GaAs stripes takes place laterally, while the vertical growth is stopped by the top dielectric cap layer. A native SiO_2 layer—due to the oxidation of the silicon substrate during the underetching step—acts as a passivating layer, avoiding parasitic nucleations of GaAs. This technique leads to nearly defect free layers because the type II dislocations (tilted 60° with respect to the substrate plane), initially present in the seed, cannot propagate beyond 1–2 μm from the seed sidewall, being blocked by the two confining layers (Si substrate and dielectric cap layer), which act as effective defect filters.

Transmission electron microscopy (TEM) showed that this growth technique leads to dislocation densities below 10^3–10^5 cm^{-2} [7], some orders of magnitude lower than those obtained on GaAs directly grown on Si. The luminescence of the conformal layers was comparable to that observed for homoepitaxial GaAs layers.

Doping of the conformal layers was also achieved by simply changing the components of the precursors. In that way, it was possible to produce n-type doped samples using Sylane as a dopant agent, with accurate control of the doping concentration over a wide range (10^{16}–10^{19} cm^{-3}).

In spite of the high quality of the GaAs/Si conformal layers some detrimental features in the layers obtained by this procedure have been observed by previous Raman and CL studies, such as the existence of strain modulations [8], the appearance of a doped stripe near the seed in unintentionally doped layers [8, 9] or the formation of Si-based complexes in the doped regions [10]. In particular, the presence of such complexes is expected to reduce the effective free carrier concentration, also producing a decrease of the carrier mobility, which would negatively affect the transport properties of the devices. For these reasons, a detailed analysis of such obstacles is very important to improve the growth procedure. In this paper, a deep analysis of the Si complex formation in the conformal layers is carried out by means of cathodoluminescence (CL) studies in the SEM.

2. Experimental and sample details

Conformal GaAs layers were grown on Si substrates following the above-described procedure. Both nominally undoped and Si-doped conformal layers were grown by HVPE at 730 °C on (100) Si substrates using gaseous GaCl and As_4 precursors for the growth of GaAs and adding SiH_4 for Si doping. The growth rate was of about 8 μm h^{-1}. Typical layers of 40 μm width

were prepared. Doped and non-intentionally doped (ND) stripes were grown just by opening and closing the aperture of the SiH_4 precursor source. The capability to obtain an accurate control of the width of the different stripes was tested by varying the SiH_4 fluence. The layer thickness was determined by the height of the cavity formed between the Si substrate and the capping dielectric layer; typically it was around 1 μm. For this study we focused on two conformal samples, referred to as CL6(K) and M422. Sample CL6(K) is a ND layer with a total width of about 40 μm. Sample M422 contains nine intentionally doped (ID) and ND intercalated stripes, although we will focus only on the first three stripes, starting from the seed, with a sequence ND/ID/ND; their widths are 7.8, 4.9 and 4.5 μm, respectively, with a donor concentration in the doped stripe of 3×10^{18} cm^{-3} (this refers to nominal values).

CL measurements were performed with the use of two systems. The first one is a Gatan MonoCL2 system installed on a Cambridge 360 Stereoscan SEM with two detectors, a Multi-Alkaly PMT with a spectral range from 300 to 900 nm, and a Ge detector with a spectral range from 800 to 1700 nm. The second one is a Gatan XiCLOne system on a JEOL JSM820 SEM in which the detection can be done with either a CCD camera (spectral range from 200 to 1000 nm), a Multi-Alkaly PMT or a Ge detector, both with similar spectral ranges as reported above. The CCD camera allows CL spectral imaging, which consists of the acquisition of a CL spectrum at each pixel of the selected measured area. From the CL spectral images we can extract monochromatic images, single spectra at selected points, the spatial distribution of the peak wavelength, profiles, etc. In both cases the measurements were done at liquid nitrogen temperature (~80 K). The electron beam energy (E_b) was selected between 4 and 20 keV with the possibility to measure the effective injection current (I_b) in the first system by using a Faraday cup. The use of these two systems with the different set of detectors is motivated by their different capabilities. The CCD camera in the second system has great advantages; in particular it allows us to easily monitor the lateral distributions of the CL emission bands, although for this study it has the disadvantage of the spectral range, covering only a short part of the infrared region. On the other hand, the use of a Ge detector allows for the accurate observation of the IR bands. The first system also allows for an accurate control of the effective injection current (I_b), thus with the possibility to carry out studies keeping the power per unit volume constant.

3. Results

By previous Raman and CL studies it was possible to reproduce accurately the doping profiles of the samples under study. For the ID stripe of sample M422 studied here, the free electron concentration and the free carrier mobility obtained from the Raman data were $3.7 \pm 0.2 \times 10^{18}$ cm^{-3} and 2002 ± 652 cm^2 V^{-1} s^{-1}, respectively [10]. On the other hand, from the combined CL and Raman measurements, the presence of a doped stripe in ND samples has been unambiguously detected [9]. This was detected for most of the conformal layers. The origin of such a doped stripe was assigned to an Si contamination from the substrate in the regions nearby the seed, due to the presence of dislocations in this area, which run away 1 or 2 μm from the seed before being stopped [9]. It is interesting to observe that the free electron concentration in these regions reaches values of about 2×10^{18} cm^{-3}, but moderated electron mobilities of about 900 cm^2 V^{-1} s^{-1} are reached.

Figure 1 shows the CL results obtained for a conformal layer with nine different doped and undoped stripes (sample M422). Figure 1(a) shows the panchromatic CL (PanCL) image as obtained with a PMT detector (15 keV, 5 nA, $T = 80$ K). Since the far-infrared region is not observable with this detector, this PanCL image nearly corresponds to the near band gap (NBG) emission image from GaAs. The GaAs seed side is indicated for clarity. As observed,

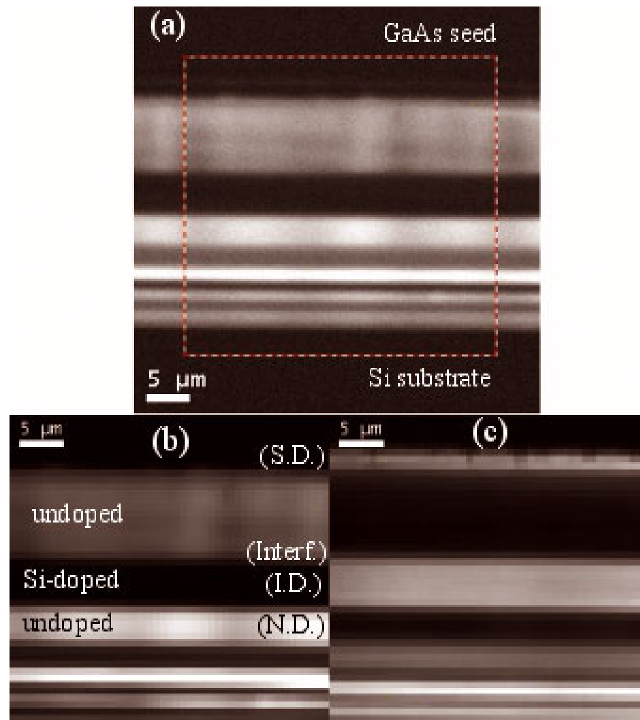

Figure 1. (a) Panchromatic CL image (taken at 15 keV) of a conformal sample with different doped and undoped stripes. The GaAs seed side is indicated for clarity; (b) and (c) monochromatic CL spectral images (at 15 keV) of the dashed area (indicated in (a)) at $\lambda = 840$ and 1000 nm, respectively.

no emission at all is detected from the seed, while the GaAs conformal layer is characterized by a high luminescence emission. The presence of the different doped and undoped stripes and their lateral extensions (matching quite well with the nominal values) is clearly observed from this PanCL image. Regarding this sample we will focus only on the first three stripes, the closest ones to the GaAs seed. Figures 1(b) and (c) show monochromatic CL images, at $\lambda = 840$ and 1000 nm respectively, obtained from a CL spectral image (CCD detector). As observed, the monochromatic CL image at 840 nm nearly matched the PanCL image obtained with the PMT detector. However, the monochromatic CL image at $\lambda = 1000$ nm, which is anticorrelated to the 840 nm one, shows clearly the presence of a bright stripe near the GaAs seed. This stripe corresponds to the above-mentioned self-doped (SD) region [9].

The use of a CCD camera on CL measurements allows us to collect simultaneously a high amount of spectral data; full spectral information of each pixel is stored. Figure 2(a) shows some of the characteristic CL spectra, extracted from the CL spectral image, at regions (SD), (ID) and (ND), as indicated in figure 1(b), corresponding to the SD, Si-doped and undoped regions, respectively. The CL spectrum of the undoped regions, (ND), shows only a very strong peak at approximately 850 nm ($\sim$1.46 eV), corresponding to the NBG emission of GaAs at this temperature. On the other hand, the CL spectra at regions (ID) and (SD), corresponding to the ID and SD regions, show a very small peak, blue shifted, in the NBG range, and a very strong band centred at approximately 1000 nm. The blue shift of the NBG is due to conduction band filling (Burstein–Moss effect [11]). The broad band has been attributed to the presence

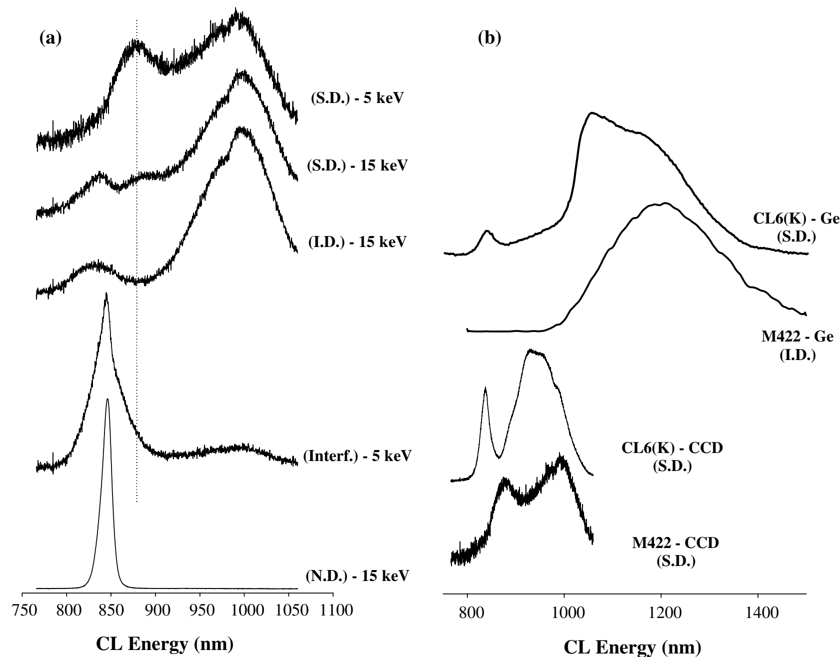

Figure 2. (a) CL spectra recorded at 15 keV at regions (SD), (ID), and (ND) as indicated in figure 1(b). The CL spectra obtained at 5 keV in the (SD) and (Interf) regions are also shown for comparison. (b) Bottom: CL spectra recorded with the CCD camera at the (SD) region of samples M422 and CL6(K) at 5 and 10 keV, respectively. Upper part: CL spectra recorded at the (SD) region of sample CL6(K) and in the (ID) region of sample M422 with the Ge detector at 10 keV.

of Si-related defect complexes [12–15]. This emission has been mainly related to the presence of Si_{Ga}–V_{Ga} complexes [12].

The observation of the same CL broad band in both ID and SD regions confirms that Si doping occurs in the SD areas. As previously discussed [9] this Si doping is likely to occur due to Si diffusion from the substrate, allowed by the dislocations present in the regions of the layer close to the seed, which is the dislocation filter zone. However, some spectral differences between ID and SD regions were also observed. A more marked blue shift of the NBG and a higher intensity of the broad band at 1000 nm were observed for the ID region, likely indicating a higher concentration of Si_{Ga}–V_{Ga} complexes in the ID layers. Another important difference concerns the presence of an additional broad band centred at approximately 875 nm ($\sim$1.42 eV) only for the SD regions, probably indicating some differences between the structures of the complexes in these regions with respect to the ID areas. The origin of this band is not clearly understood at present. Some luminescence bands have been observed at such a low wavelength, and they were related to Si_{Ga}–Ga_{As} complexes [13].

The same analysis was performed for this sample at lower electron beam energy (5 keV) aiming to obtain a rough picture of the in-depth distribution of the Si complex. The maximum penetration depth (R_e) of the primary electrons in GaAs at 5 and 15 keV corresponds to 0.16 and 0.90 μm, respectively. The CL spectra taken at the same point inside the SD region for both electron beam energies are shown in figure 2(a). The band centred at 875 nm is more intense at 5 keV and seems to be in competition with the band centred at 1000 nm. This supports the above-mentioned existence of more than one type of complex in the SD region. The monochromatic CL spectral images at 875 and 1000 nm taken at 5 keV are also shown

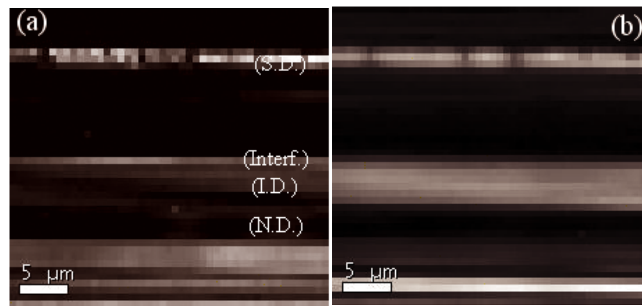

Figure 3. Monochomatic CL images at $\lambda = 875$ nm (a) and $\lambda = 1000$ nm (b) of the same region of the conformal layer as shown in figure 1 taken at $E_b = 5$ keV.

for comparison in figure 3. The transition at 875 nm only concerns the SD areas (see the CL spectra at regions (SD) and (ID)) and is mainly concentrated in the closest regions to the seed; see figure 3(a). The bright halo observed in some regions of the conformal layers in figure 3(a), as in the interfaces between the ND and ID stripes, corresponds to band tails of the broad NBG emission of the (ID) stripe. This is shown in the CL spectrum obtained at the interface, figure 2(a).

A more detailed analysis of the Si complex related emission has been performed using a Ge detector. Figure 2(b) plots the CL spectra obtained for sample CL6(K) in the self-doped region, using both the CCD camera and the Ge detector, at an electron beam energy of 10 keV at 80 K, as well as the CL spectra obtained for sample M422 with the Ge detector in the studied doped stripe (ID) at 10 keV and with the CCD camera in the self-doped region (SD) at 5 keV. The comparison between the CL spectra acquired with the CCD camera in the self-doped regions for the two samples allows us to establish some similarities and differences. The NBG emission is more intense in the SD region of sample CL6(K). About the broad bands related to the Si complexes, sample CL6(K) exhibits the main band at about 950 nm, with shoulders at 890 and 1000 nm, corresponding to the bands observed in sample M422. On the other hand, the observed difference between the CL spectra obtained on the self-doped region of sample CL6(K) with both the CCD camera and the Ge detector in the band centred at 1000 nm could be due to the CCD spectral response in this range. New complexes related bands in the range 1000–1200 nm become evident, when observed with the Ge detector. Similar bands are observed in the CL spectrum of the doped stripe of sample M422 obtained with the Ge detector, which shows a broad band in the IR region between 1000 and 1400 nm. This broad band should involve more than one transition. The CL spectra acquired with the use of the Ge detector, for different conformal samples in both SD and ID stripes, have always shown broad bands formed of several components. Deconvolution of the CL spectrum obtained in the SD region of sample CL6(K), figure 2(b), reveals three main bands peaking at 950 nm ($\sim$1.31 eV, here denoted as P1 emission), 1035 nm ($\sim$1.19 eV, P2 emission) and 1100 nm ($\sim$1.12 eV, P3 emission), accounting for the existence of several Si complexes. These bands have been reported in the literature and were related to Si_{As}–V_{As} for the P1 emission [14], Si_{As}–V_{Ga} for the P2 emission [12] and Si_{Ga}–Si_{As} for the P3 emission [15].

Depth-resolved CL analyses were carried out to investigate the in-depth distribution of the different Si-related complexes. This study was performed with an accurate control of the effective current injection (I_b). A series of CL spectra at different electron beam energies (from 6 to 16 keV) was recorded with the Ge detector in the SD region of sample CL6(K) by keeping constant the power per unit volume ($I_b E_b / R_e$). Here R_e means the penetration depth, which

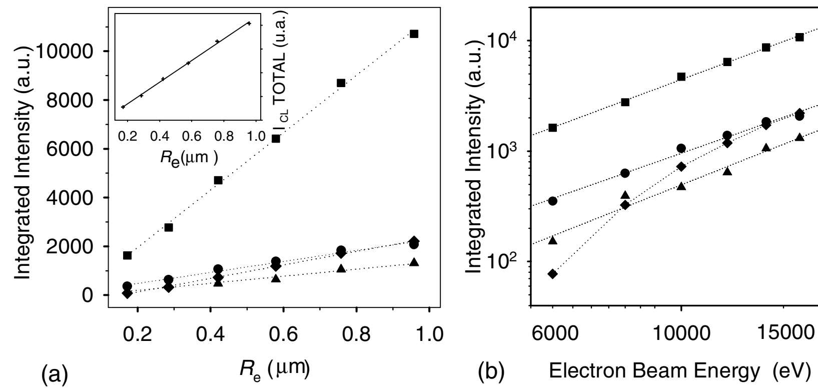

Figure 4. (a) Integrated intensity of the different CL peaks observed in the SD region of sample CL6(K) as a function of the penetration depth (the inset shows the total integrated intensity); (b) integrated intensity (logarithmic scale) of the different CL peaks as a function of the electron beam energy. (rhombus: NBG emission; triangles: P1 emission; circles: P2 emission; squares: P3 emission).

has been calculated according to the equation of Kanaya and Okayama [16]. This warrants that the number of generated electron–hole pairs is nearly constant, thus, providing a quantitative picture of the in-depth CL intensity and therefore of the depth distribution of Si complexes. Sample CL6(K) was selected due to the observation of the NBG emission, which would allow to normalize the Si-related bands.

The integrated intensity of the different peaks changes as a function of the electron penetration depth, as shown in figure 4(a). The peak intensities increase linearly as a function of the penetration depth in the selected range of electron beam voltages, which guarantees we are working inside the SD region. The higher increase of the P3 peak intensity with respect to the other ones should mean that the concentration of centres responsible for this luminescence increases with depth. Figure 4(b) shows the peak intensities (logarithmic scale) as a function of the electron beam energy. Apart from the NBG emission, which the intensity decreases as the surface is approached, likely due to the presence of surface states, the three Si-related peaks show a similar linear dependence with the e-beam voltage.

The logarithmic dependence of the integrated intensity versus the beam current for the peaks corresponding to the SD region of sample CL6(K) shows a sublinear dependence, $I_{\mathrm{CL}} = K I_{\mathrm{exc}}^{b}$, where the parameter b is indicative of the recombination mechanism; see figure 5. The values obtained for peaks P2 and P3, 0.67 and 0.51 respectively, are typical of donor acceptor pair (DAP) transitions. The peaks corresponding to the NBG and P1 transitions could not be analysed because their intensities for low injection currents were very poor, and the results obtained were not enough reliable.

4. Conclusions

Different Si defect related emissions have been observed in conformal GaAs on Si layers in both ID and SD regions. The same nature of some transitions in both regions confirms that Si is the main dopant in the SD areas. However, some clear differences between SD and ID regions were also observed using spectral imaging, which allowed us to characterize the spatial distribution of complexes. In particular, the presence of a broad band at 875 nm was preferentially observed in the upper part of the SD stripe and very close to the seed. On the

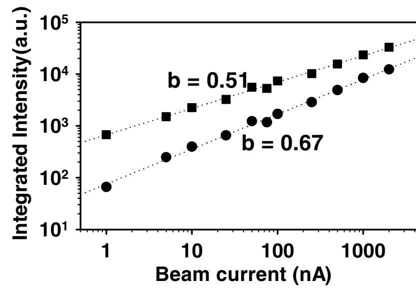

Figure 5. The dependence of the intensity versus I_{exc} for P2 (squares) and P3 (circles) emissions obtained in the self-doped region on sample CL6(K).

other hand, broad bands with different peaks in the range 950–1400 nm were observed in all the doped regions, indicating a complex character with more than one Si defect related pair. By means of power-dependent and depth-resolved CL studies it was possible to relate them to DAP transitions and to observe differences in the in-depth distribution of the different Si complexes.

References

[1] Egawa T, Jimbo T and Umeno M 1993 *Japan. J. Appl. Phys.* **32** 650
[2] Yodo T and Tamura M 1995 *Japan. J. Appl. Phys.* **34** 3457
[3] Fang S F, Adomi K, Iyer S, Morkoc H, Zabel H, Choi C and Otsuka N 1990 *J. Appl. Phys.* **68** R31
[4] Kuz'menko R V, Ganzha A V, Bochurova O V, Domashevskaya E P, Schreiber J, Hildebrandt S, Mo S, Peiner E and Schlachetzki A 2000 *Semiconductors* **34** 73
[5] Zytkiewicz Z R 1999 *Cryst. Res. Technol.* **34** 573
[6] Pribat D, Provendier V, Dupuy M, Legagneux P and Collet C 1991 *Japan. J. Appl. Phys.* **30** L431
[7] Pribat D, Gérard B, Dupuy M and Legagneux P 1992 *Appl. Phys. Lett.* **60** 2144
[8] Ardila A M, Martínez O, Avella M, Jiménez J, Gil-Lafon E and Gérard B 2002 *J. Mater. Res.* **17** 1341
[9] Ardila A M, Martínez O, Avella M, Jiménez J, Gérard B, Napierala J and Gil-Lafon E 2001 *Appl. Phys. Lett.* **79** 1270
[10] Ardila A M, Martínez O, Avella M, Jiménez J, Gérard B, Napierala J and Gil-Lafon E 2002 *Mater. Res. Soc. Symp. Proc.* **692** 417
[11] Burstein E 1954 *Phys. Rev.* **93** 632
[12] Visser E P, Tang X, Wieleman R W and Giling L J 1991 *J. Appl. Phys.* **69** 3266
[13] Harrison I, Pavesi L, Henini M and Johnston D 1994 *J. Appl. Phys.* **75** 3151
[14] Hong Ky N, Pavesi L, Araújo D, Ganière J D and Reinhart F K 1991 *J. Appl. Phys.* **70** 3887
[15] Fujii K, Okada Y and Osito F 1993 *J. Appl. Phys.* **73** 88
[16] Kanaya K and Okayama S 1972 *J. Phys. D: Appl. Phys.* **5** 43